Colloid Polym Sci (2002) 280: 653–660
DOI 10.1007/s00396-002-0670-7

ORIGINAL CONTRIBUTION

Haifeng Gao
Yiqiang Zhao
Shoukuan Fu
Bin Li
Minqian Li

Preparation of a novel polymeric fluorescent nanoparticle

Received: 12 November 2001
Accepted: 28 January 2002
Published online: 24 April 2002

H. Gao · Y. Zhao · S. Fu (✉)
Department of Macromolecular Science, and the Key Laboratory of Molecular Engineering of Polymers, Ministry of Education, Shanghai, 200433, China
E-mail: skfu@srcap.stc.sh.cn

B. Li · M. Li
Shanghai Institute of Nuclear Research, Chinese Academy of Science, Shanghai, 201800, China

Abstract A new type of narrowly dispersed fluorescent crosslinked polystyrene (PS) nanoparticles (20–50 nm) was synthesized via a modified microemulsion copolymerization of styrene, crosslinker divinyl benzene (DVB) and a hydrophilic comonomer amino ethyl methacrylate hydrochloride (AEMH), in the presence of pyrene. Characterized by steady-state fluorescence spectra, these nanoparticles show high luminescent intensity and the embedded pyrene has a negligible desorption from the nanoparticles. The emission intensity I_1 of the pyrene in the crosslinked nanoparticles is 40 times higher than that of pyrene in toluene or styrene solution with the same concentration. The fluorescence emission intensity can be varied by the amount of the monomer, crosslinker and pyrene, but is influenced little by the amount of AEMH in the range of investigation. The surface of the nanoparticles is modified by amino and amidino functional groups introduced by the comonomer and the initiator 2, 2′-azobis (2-amidinopropane) dihydrochloride (V_{50}), which controls the zeta potential on the particle surface.

Keywords Polymeric nanoparticles · Fluorescence · Pyrene · Zeta potential

Introduction

Recently, fluorescent particles have become widely used tracers in many different applications, especially in the biological fields, such as immuno and genetic fluorescence detection [1, 2, 3], neuroscience and cell labeling in vitro and in vivo [4], pharmaceutical delivery [5], and in situ hybridization [6]. The fluorophores trapped in the particles avoid the photo instability caused by the direct coupling between the dye molecules and the probed parts [7].

To date, there have been developed several kinds of particles as fluorescent probes, where semiconductor nanocrystals have received great attention [8, 9, 10]. Due to the quantum confinement effect, nanocrystals which combine the physical and chemical properties of molecules with the optoelectronic properties of semiconductors [11] have become a rapidly growing subjects in chemistry and physics. The fluorescent nanoparticles are suitable for the biomarker applications since they are much smaller than cells and have a similar size as biological molecules [12]. Recently, a layer-by-layer method has been employed to synthesize fluorescent microparticles by depositing multiple layers of polyelectrolytes on a pyrene microcrystal template. The adsorption and desorption of the pyrene molecules have been studied systematically [13].

Many researches on trapping fluorophores to the metallic, zeolite or polymeric particles have also been published in the last few years [14, 15]. With the polymeric materials as the matrices to prepare fluorescent particles, polystyrene and polyalkylcyanoacrylate particles have received special recognition [16, 17, 18]. However, so far, most of the fluorescent particles have been prepared by physical adsorption or covalent binding to connect the fluorophores to the vehicles. The

majority of the dyes existing on the particle surface layer are unstable when varying the environment. Apart from the low adsorption amount, dye desorption limits the utility of such particles [15, 17].

In this paper, an alternative method is presented, and a modified microemulsion polymerization procedure [19, 20] is used to prepare novel fluorescent polystyrene nanoparticles. Pyrene used here as the fluorophore has a long singlet lifetime, and the vibrational band structure of its emission is sensitive to the environment. It is by far the most frequently used dye in fluorescence studies of labeled polymers [21]. We show that the fluorescent micropartcles have nanosize (20–50 nm) dimensions and the pyrene molecules with a high luminescence intensity are embedded in the hydrophobic PS cores. Compared with the conventional method where fluorophores are adsorbed on the particle surface, this one-step copolymerization procedure leads to a deep embedding of the fluorophores into the nanoparticles. With the reactive functional groups of amino and amidino on the particle surface, the fluorescent polymeric nanoparticles could be easily covalently bound to proteins, oligonucleotides, or cells, acting as a useful biological marker in many applications.

Experimental

Materials. Styrene (St) and divinyl benzene (DVB, 55%, TCI) were distilled under reduced pressure before polymerization. 2, 2′-Azobis(2-amidinopropane) dihydrochloride (V_{50}, 99.5%, Aldrich), pyrene (99%, Aldrich), amino ethyl methacrylate hydrochloride (AEMH, 99%, ACROS), polyethylene glycol monononylphenyl ether (NP-40 and NP-9, both 99%, Henkel) were all used as received. Deionized water was used for all experiments.

Preparation of fluorescent polymeric nanoparticles. A typical example (D2) is described as follows. A transparent microemulsion composed of 0.35 g St, 5 mg pyrene, 2.25 g NP-40, 0.25 g NP-9, and 38 g water was added to a 100-ml three-neck flask equipped with a reflux condenser, a thermometer, two dropping funnels, a nitrogen gas inlet and outlet, and a magnetic stirring bar. The microemulsion was heated to 60 °C for 15 min with nitrogen bubbling, then to 80 °C. After 10 min, a solution of 0.0271 g V_{50} in 3 g water was added to initiate the polymerization of the slightly bluish microemulsion. After 10 min, a mixture of 2.65 g St and 0.075 g DVB was added dropwise (15 s/drop) into the microemulsion through a dropping funnel. When half of the mixture had been added, a solution of 0.1 g AEMH in 3 g water was added dropwise (8 s/drop) to the polymerizing system through the other funnel. During addition, the temperature was kept at 80 ± 2 °C, a slow flow of nitrogen maintained and the reacting mixture was stirred with a magnetic bar. After the addition of monomers, the stirring as well as the temperature and nitrogen flow was kept going for another 3 h essentially to complete the conversion of the monomers. Other microlatices were polymerized by a similar procedure. Generally, the monomer conversion was higher than 95% [20].

Purification of fluorescent polymeric nanoparticles All the nanoparticles were cleaned via nanofilter operations to remove the hydrophilic homopolymer poly(AEMH) and the excess surfactants from the microlatices system. Under nitrogen pressure (0.3 MPa) and magnetic stirring, filter liquor containing the homopolymer and excess surfactants passed slowly through the nanofilter films (MW cutoff = 10^5 g/mol^{-1}). This process was repeated until the results of GPC measurement of the filter liquor had no trace of them. Determined from GPC results, the amount of the homopolymer in the microlatices is about 5 wt% of the total hydrophilic comonomer of AEMH added.

Characterization of the fluorescent polymeric nanoparticles. Various techniques were used to determine the luminescence intensity, particle imaging, dispersity, and the surface charge of the fluorescent PS nanoparticles.

Fluorescence spectra were recorded using a FZ-I steady-state fluorescence spectrometer with a right-angle geometry (90° collecting optics). The excitation and emission slits were both 5 nm wide. The measured microlatex was diluted and the final concentration contained $\sim 10^{-6}$ mol pyrene per kg of the microlatex (the content of solids was $\sim 10^{-3}$ wt%). The diluted microlatex was allowed to stand at room temperature for at least 12 h before fluorescence measurement. The excitation wavelength was 350 nm.

Quasi-elastic light scattering (QELS) measurements were carried out in standard multiangle laser light scattering equipment (Malvern 4700). The light source was a 100 mW Ar-ion laser, which produces vertical polarized light at $\lambda = 514.8$ nm. The scattering cells (103 cylindrical ampoules) were immersed in a thermostatted water bath.

Zeta potential measurements of the fluorescent nanoparticles with hydrophilic functional groups (amino and amidino) on the surface were performed using standard multiangle laser zeta potential equipment (Malvern 4700).

The fluorescence photographs were taken using a fluorescence microscope (Nikon 1800, multiple: 100, NA: 1.3). The analytical tool is a thermoelectrically cooled charge-coupled device (CCD) detector from Princeton Instruments Inc.

Transmission Electron Micrographs (TEM) were obtained using the Hitachi H-600 transmission electron microscope. Clusters of closely spaced particles were mainly formed by sample spreading and dried on the copper grid. On different sites of the TEM photographs, the diameters of more than 100 individual particle were measured, and the average size and the coefficient of variation (CV) were obtained from

$$\bar{D} = \frac{\sum_{i=1}^{n} D_i}{n};\ S = \sqrt{\frac{\sum_{i=1}^{n} (D_i - \bar{D})^2}{n-1}};\ CV(\%) = S/\bar{D} \times 100\% \qquad (1)$$

where $\bar{D}$ is the number average diameter, D_i is the diameter of the particle i, n is the total number counted, and S is the particle size standard deviation.

Results and discussion

The fluorescent microlatices were synthesized through a modified microemulsion copolymerization of the hydrophobic monomer St, crosslinker DVB, and the hydrophilic comonomer AEMH. Thus the nanoparticle has a core-shell structure with a crosslinked PS core and a poly(AEMH) shell (see later). The detailed recipes for various fluorescent microlatices are listed in Table 1. The particle size determined by QELS doesn't change much with the amount of the added AEMH, but does change with the amount of St and DVB used. Since the microlatices are mainly stabilized by the surfactants (NP-40 and NP-9), the amount of the added hydrophilic comonomer AEMH doesn't have an evident effect on the particle size in the range of investigation.

Table 1. Polymerization recipes for various fluorescent nanoparticles

Exp. No.[a]	Monomer (g)[b]			Pyrene (mg)[c]	Particle size (nm)[d]
	St	DVB	AEMH		
D1	3.0	0.033	0.100	5.00	37.3
D2[e]		0.075			35.5
D3		0.125			43.0
D4		0.203			46.2
D5		0.297			47.1
P1	3.0	0.075	0.100	2.48	34.9
P2				5.00	35.5
P3				6.85	39.7
P4				9.45	37.3
P5				17.79	38.9
M1	2.0	0.050	0.200	5.00	29.0
M2	3.0	0.075			38.1
M3	4.0	0.100			53.2
M4	5.0	0.125			72.6
A1	3.0	0.075	0	5.00	37.3
A2			0.026		36.5
A3			0.052		38.0
A4			0.080		38.6
A5			0.100		35.5
A6			0.150		35.0
A7			0.200		38.1

[a]All the microlatices had a surfactant amount of 2.25 g NP-40 and 0.25 g NP-9, the initiator was V_{50} and the amount was 0.0271 g

[b]Among the added amount of St, 0.35 g was mixed with pyrene, surfactant, and 38 g water to form a transparent microemulsion before polymerization. The rest amount of St and all the DVB were mixed and added dropwise in the reacting microemulsion 10 min after the polymerization began. After half of the mixture was added, a solution of 0.1 g AEMH in 3 ml water was added dropwise into the polymerizing system

[c]All the pyrene was dissolved in 0.35 g St to form a transparent microemulsion with all the surfactant and 38 g water before polymerization

[d] the particle sizes are hydrodynamic volume measured with the quasi-elastic light scattering before the nanofilter process

[e]D2 is also named P2, A5

Steady-state fluorescence measurements

Pyrene, a widely used fluorophore, is sensitive to environmental polarity. When transferred from a polar to a nonpolar environment, the photophysical properties, such as the quantum yield, the vibrational structure reflected in the intensity ratio (I_1/I_3) of the first and third bands in its emission spectrum change remarkably [22, 23, 24]. Figure 1 shows the fluorescence emission spectra of various microlatices diluted from the sample of D2. The peaks of I_1 and I_3 appear at 375 nm and 386 nm, respectively (Fig. 1A), which is consistent with the fluorescence spectra of pyrene in bulk PS [25]. While increasing the pyrene concentration, the intensity of the peak I_1 increases linearly (Fig. 1B). Because both pyrene and polystyrene are high hydrophobic, when the polymerization occurs in the aqueous medium, pyrene molecules are preferably embedded into the hydrophobic core of the nanoparticles instead of being homogeneously dispersed in the microlatex system. Compared with the fluorescence emission intensity I_1 of pyrene in the solution with toluene or styrene as solvent (Fig. 1B, inset), the emission intensity of pyrene in the microlatex with the same concentration is nearly 40 times higher. Since the pyrene molecules are embedded in the crosslinked PS nanoparticles, their fixed location in the crosslinking network reduces the interaction and quenching of the excited pyrene molecules with other molecules [25].

As consequence of concentration, the microlatices diluted from the sample of D2 either before or after the nanofilter process have nearly the same fluorescence emission intensity (Fig. 1B). Combined with the linear change of the fluorescence intensity I_1 with the pyrene concentration, this proves that neither the nanofilter process nor the dilution process can make the pyrene molecules escape from the nanoparticles.

Changing the pyrene concentration, the intensity ratio (I_1/I_3) doesn't change much from a value of about 1.05 (Fig. 1C), which is similar to that of pyrene in PS films (0.95) [24]. According to earlier reports [22, 23], the intensity ratio (I_1/I_3) of pyrene is sensitive to the polarity of the medium, which can change from a value of 1.9 in the medium of water to 1.0 in anionic surfactant micelles or even 0.62 in cyclohexane [24]. Since I_1/I_3 in the microlatice is similar to that in a PS film but much lower than in water, most of the pyrene molecules must be embedded in the hydrophobic PS core of the nanoparticles.

Figure 2 shows the dependence of the fluorescence intensity I_1 and the intensity ratio (I_1/I_3) of pyrene on

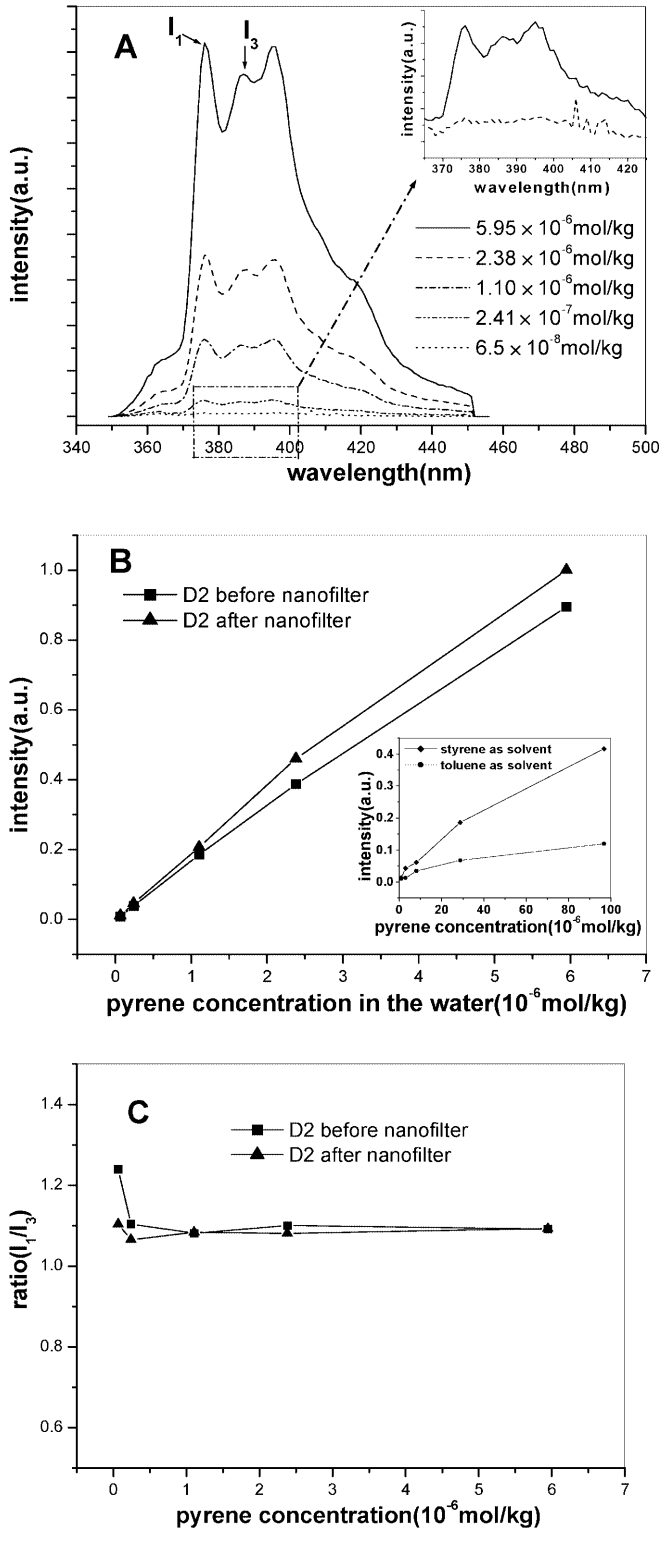

Fig. 1A–C. Fluorescence emission spectra of various microlatices diluted from the sample of D2 with the excitation at 350 nm: **A** the emission spectra of various microlatices with different pyrene concentration before nanofilter process, the *inset* is the amplified spectra; **B** the intensity of the peak I_1 of each spectra in A as a function of the pyrene concentration, the *inset* is the intensity I_1 of pyrene in the solution as a function of the pyrene concentration with toluene or styrene as solvent; **C** I_1/I_3 as a function of the pyrene concentration. All the spectra were normalized

the weight ratio of the added DVB/St (Table 1, D1∼D5). Increasing the weight ratio of DVB/St, the fluorescence intensity I_1 and the intensity ratio (I_1/I_3) both decrease slightly. With more DVB used as crosslinker, the crosslinking density becomes higher and the PS core is stiffer. Thus the polarity of the environment around the excited pyrene molecules decreases, which induces I_1/I_3 to decrease slightly. However, with more DVB used, the fluorescence intensity I_1 also decreases about 10%. Compared with the constant fluorescence intensity with various DVB used in bulk PS [25], this result is confusing. With more DVB added, the structure of the fluorescent nanoparticles becomes more complicated, so the distribution of the embedded pyrene molecules in the crosslinked nanoparticles and the microenvironment around seem both to be affected. These factors may be part of the reasons for the decreasing intensity with an increase of added DVB.

Figure 3 shows the pyrene concentration dependence of the fluorescence intensity I_1 and the intensity ratio (I_1/I_3) (Table 1, P1∼P5). With an increasing pyrene concentration, the fluorescence intensity increases linearly. Since the microlatices have the same content of solids and nearly the same particle size, this indicates that nearly all the pyrene molecules are embedded in the particles in the range of investigation, and the fluorescence emission intensity could be controlled linearly by the amount of pyrene. The constant intensity ratio (I_1/I_3) shows that in the range of investigation, most of the added pyrene has been embedded into the hydrophobic core of the nanoparticles, where the polarity is stable.

Figure 4 shows the particle size dependence of the fluorescence intensity I_1 and the intensity ratio (I_1/I_3) (Table 1, M1∼M4). When more St and DVB is added, a larger particle size is obtained. Calculating from the data shown in Table 1, the number of the pyrene molecules embedded into each crosslinked nanoparticle increases with the particle size, while the whole particle number decreases (Table 2). With a constant amount of pyrene in the microlatex system, the enrichment of more pyrene molecules in the larger particles enhances the emission intensity. On the other hand, with a constant amount of pyrene added, the higher content of solids leads to a dilution of the pyrene molecules in the crosslinked PS particles. Thus the interaction and quenching of the excited pyrene with other molecules decrease, which could also cause an increase in the fluorescence emission intensity. Moreover, with the particle size increasing, the polarity of the environment around the pyrene molecules remains stable, as demonstrated by the unchanging I_1/I_3.

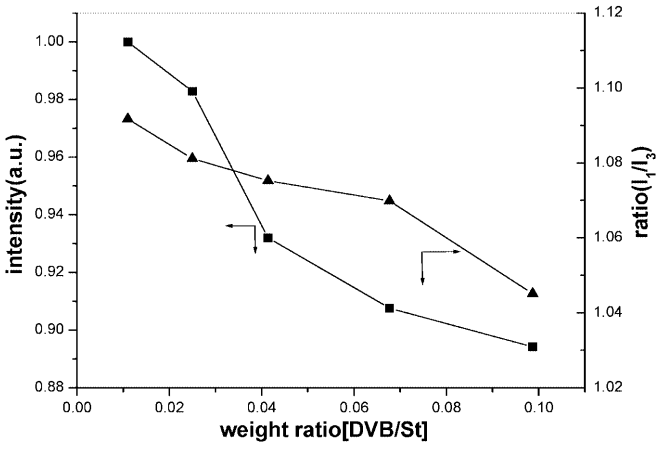

Fig. 2. The dependence of I_1 and I_1/I_3 on the weight ratio of the added DVB/St (Table 1, D1∼D5), all the microlatices for measurement had been diluted to 1.10×10^{-6} mol/kg of pyrene in the microlatex; the used spectra were normalized

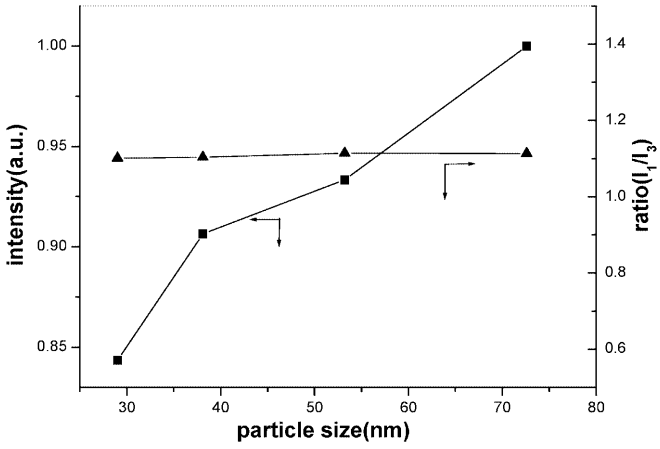

Fig. 4. The particle size dependence of I_1 and I_1/I_3 (Table 1, M1∼M4); all the microlatices for measurement had been diluted to 1.10×10^{-6} mol/kg; the used spectra were normalized

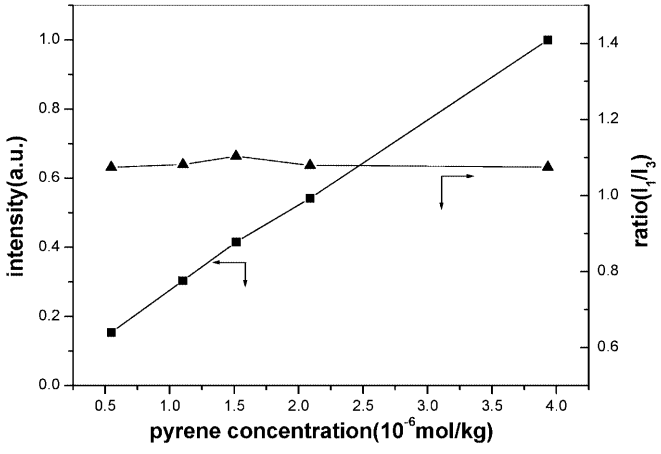

Fig. 3. The pyrene concentration dependence of I_1 and I_1/I_3 (Table 1, P1∼P5); all the microlatices for measurement had been diluted to the same content of solids; the used spectra were normalized

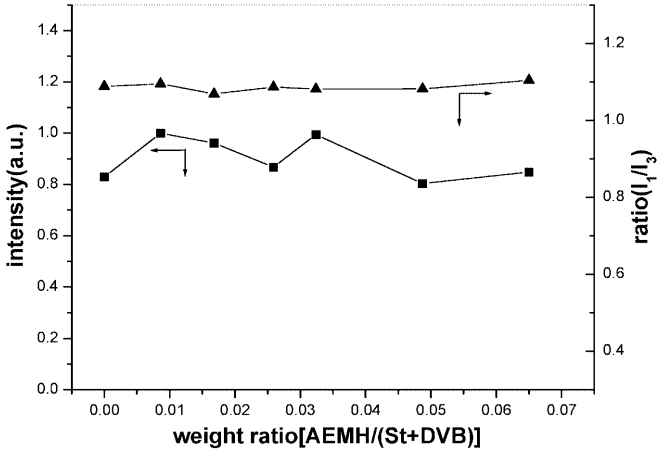

Fig. 5. The dependence of I_1 and I_1/I_3 on the weight ratio of AEMH/(St and DVB) (Table 1, A1∼A7); all the microlatices for measurement had been diluted to 1.10×10^{-6} mol/kg; the used spectra were normalized

Figure 5 shows the dependence of the fluorescence intensity I_1 and the intensity ratio (I_1/I_3) on the weight ratio of the added AEMH/(St and DVB) (Table 1, A1∼A7). Increasing the added amount of hydrophilic comonomer AEMH, the intensity I_1 and the intensity ratio (I_1/I_3) remain nearly unchanged. This shows that in the range of investigation, the added comonomer AEMH is mostly located at the surface or shell of the

Table 2. The whole particle number of the microlatex (N), the average number of pyrene molecules embedded into one nanoparticle (n) and the overall surface area varied with the content of solids (Table 1, M1∼M4)

Exp. No.[a]	Solids content[b] (g)	Particle size (nm)	N ($\times10^{17}$)	n ($\times10^{5}$)	Overall surface area (m^2)
M1	4.750	29.0	3.72	0.28	982.76
M2	5.775	38.1	1.99	0.47	909.45
M3	6.800	53.2	0.86	1.10	766.92
M4	7.825	72.6	0.39	2.44	646.69

[a]The density of all the nanoparticles is assumed as 1 g/cm^3
[b]Which contains the whole weight of St, DVB, AEMH and surfactant

nanoparticles, which has no effect on the environmental polarity around the embedded pyrene molecules. This shows that the fluorescent nanoparticles here is a core-shell structure, where the core is composed with the hydrophobic crosslinked PS and the shell is composed of the hydrophilic poly(AEMH) and surfactants. The pyrene molecules are embedded into the central part of the hydrophobic-hydrophilic nanoparticles, so it is very difficult for them to escape from the nanoparticles.

Zeta potential measurements

Zeta potential is a concept to describe the electrokinetic property of a colloid under the influence of an applied electric field. For the nanoparticles synthesized through the same polymerization procedure with the similar recipe, the zeta potential of each nanoparticle has a proportional relation with the surface charge density of the colloid [26]. Through the copolymerization of St, DVB, and AEMH, initiated by V_{50}, the amino and amidino groups are introduced to the nanoparticle surface, which endows the colloids with positive charge in acidic conditions [27]. The zeta potential as a function of the weight ratio of AEMH/(St and DVB) is shown in Fig. 6. As elucidated above, increasing the amount of the added AEMH could not change the nanoparticle size very much, but it can influence the zeta potential, as well as the surface charge density. At 10^{-3} mol l^{-1} NaCl, and pH = 4, all the amino and amidino groups are protonized. When the comonomer AEMH is not added, the surface charge of the nanoparticle is determined by the amidino group introduced by the initiator V_{50}, with a zeta value of 17 mV. Increasing the added amount of AEMH, the zeta value increases. When the added amount of AEMH is small, the zeta value of the nanoparticles increases nearly linearly; with more AEMH added gradually, the proportion of the AEMH connected to the particles decreases, so the curve tends to level off.

Figure 7 shows the dependence of the zeta potential on the particle size (Table 1, M1∼M4). Increasing the content of solids of the microlatices, the particles become larger, but the overall surface area decreases (Table 2.). Since the added amount of AEMH and V_{50} are constant, the decrease of the overall surface area causes an increase of the amount of amino and amidino groups per surface area, which leads to a rising zeta potential. Generally, the surface charge density of the fluorescent nanoparticles can be controlled partially by adjusting the amount of the added hydrophilic comonomer. The functional amino and amidino groups could be chemically bound with the functional groups on the biological molecules, such as amino, carboxyl, hydroxyl, sulfonate, etc., presenting a practical way to utilize the fluorescent nanoparticles as a bioactive probe.

TEM and fluorescent photo measurements

Figure 8 is a TEM image of the microlatex of D2, in which, the fluorescent nanoparticles could be seen with a good dispersity on the nanoscale. Using Eq. (1), the average particle size is 20.1 nm and $CV\ (\%) = 20.5$. Compared with the particle size of the same microlatex from the QELS measurement (35.5 nm, Table 1), the particle size from TEM is considerably smaller. As some other groups reported, such a result is confirmed [28, 29],

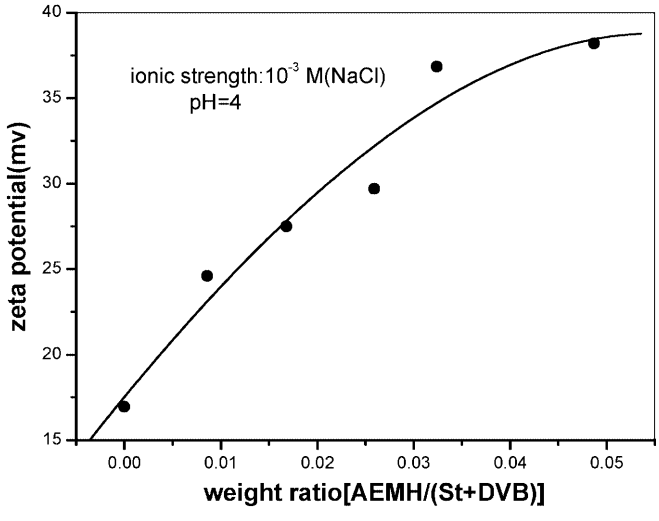

Fig. 6. Zeta potential as a function of the weight ratio of AEMH/(St and DVB) (Table 1, A1∼A7)

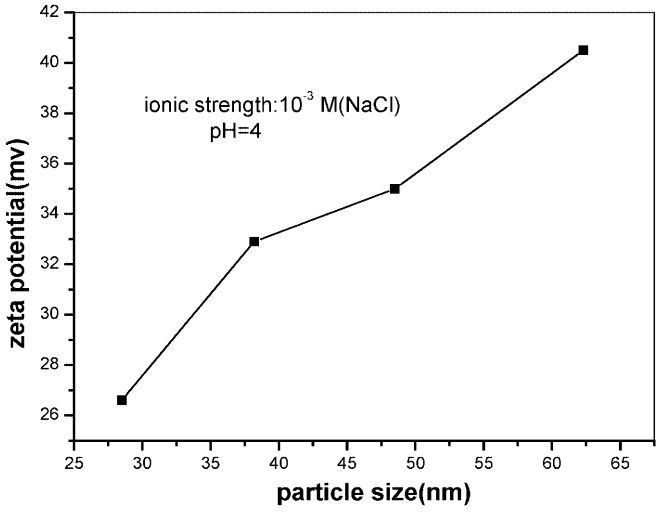

Fig. 7. Zeta potential as a function of the particle size (Table 1, M1∼M4)

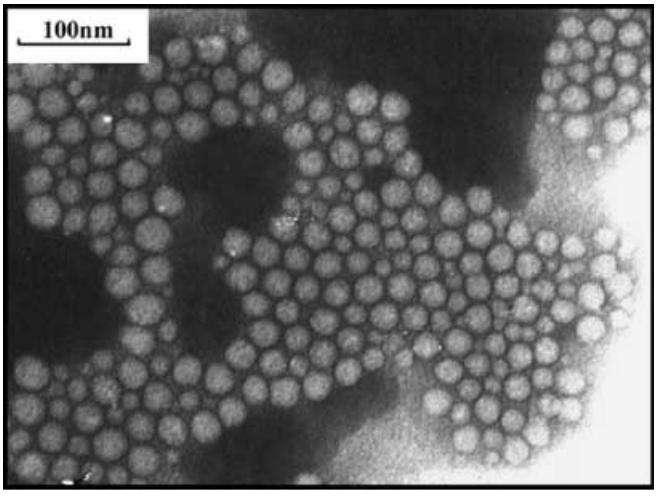

Fig. 8. TEM photograph of the microlatex D2 after repeated nanofilter process

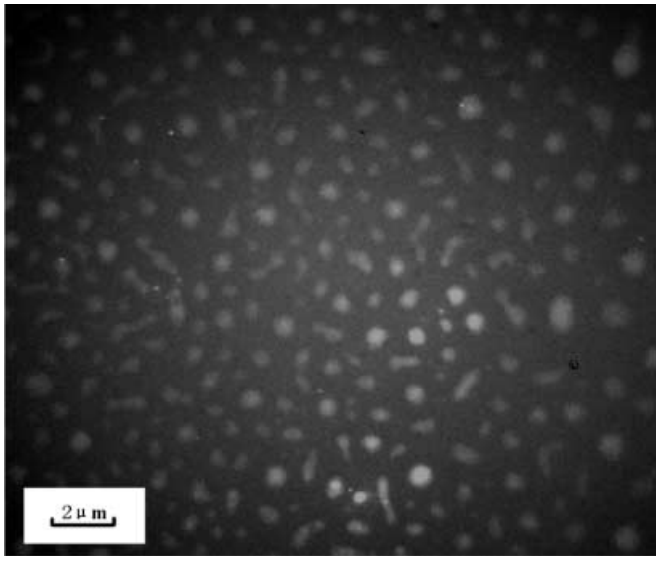

Fig. 9. Fluorescence photograph (×100) of the microlatex D2 after repeated nanofilter process

and can be explained by the presence of the hydrophilic poly(AEMH) chains on the particle surface causing the hydrodynamic volume to be larger than expected. Figure 9 shows the fluorescent photograph of the microlatex of D2, and the size of the luminescent spot shows the scale of the halo, which is therefore larger than the real size of the fluorescent nanoparticle. This image shows that the luminescent intensity is high, and the shining particles disperse very well. The goal of raising the number of fluorophores in one polymeric nanoparticle, so as to enhance the intensity of the probe, has been accomplished.

Conclusion

Core-shell polymeric nanoparticles with high fluorescence, variable zeta potential and variable size can be synthesized through the modified microemulsion copolymerization of the hydrophobic monomer St, DVB and the hydrophilic comonomer AEMH, in the presence of pyrene as fluorophore. Pyrene is incorporated in the hydrophobic core of the particles and is not released from the particles. With a series of measurements, including steady-state fluorescence spectra, zeta potential measurement, TEM, fluorescence photography, QELS, etc., the fluorescence intensity of pyrene embedded in the particles is found to be 40 times higher than that of pyrene with the same concentration in toluene or styrene solution, and could be controlled by crosslinking density and pyrene amount. With the functional amino and amidino groups, varied by the amount of functional comonomer, on the particle surface, it is possible for some biological materials to undergo coupling to the fluorescence nanoparticles.

Acknowledgements This work was supported by the National Science Foundation of China (No.29874010) and the Foundation of the Laboratory of Nuclear Analysis Techniques, Chinese Academy of Sciences (No.20035). We are also grateful for the experimental support and valuable suggestions on the steady-state fluorescence measurements by Prof. Ming Jiang's group from the Department of Macromolecular Science, Fudan University, Shanghai, China.

References

1. Hakala H, Maki E, Lonnberg H (1998) Bioconjugate Chem 9:316
2. Dubertret B, Calame M, Libchaber AJ (2001) Nat Biotechnol 19:365
3. Taylor JR, Fang MM, Nie SM (2000) Anal Chem 72:1979
4. Bhalgat MK, Haugland RP, Pollack JS, Swan S (1998) J Immunol Methods 219:57
5. Geddes CD, Apperson K, Birch DJS (2000) Dyes Pigm 44:69
6. Pathak S, Choi SK, Arnheim N, Thompson ME (2001) J Am Chem Soc 123:4103
7. Scheenen WJJM, Makings LR, Gross LR, Ozzan T, Tsien RY (1996) Chem Biol 3:765
8. Bruchez M, Moronne M, Gin P, Weiss S, Alivisatos AP (1998) Science 281:2013
9. Susha AS, Caruso F, Rogach AL, Sukhorukov GB, Kornowski A, Mohwald H, Giersig M, Eychmuller A, Weller H (2000) Colloid Surf A 163:39
10. Matsuzawa Y, Suzuki J (2001) J Chem Eng Jpn 34:700

11. Shim M, Guyot-Sionnest P (2000) Nature 407:981
12. Santra S, Wang KM, Tapec R, Tan WH (2001) J Biomed Opt 6:160
13. Yang WJ, Trau D, Renneberg R, Yu NT, Caruso F (2001) J Colloid Interface Sci 234:356
14. Makarova OV, Ostafin AE, Miyoshi H, Norris JR, Meisel D (1999) J Phys Chem B 103:9080
15. Schlupen J, Haegel FH, Kuhlmann J, Geisler H, Schwuger MJ (1999) Colloids Surf A 156:335
16. Meallet-Renault R, Denjean P, Pansu RB (1999) Sensors Actuators B 59:108
17. Charreyre MT, Zhang P, Winnik MA, Pichot C, Graillat C (1995) J Colloid Interface Sci 170:374
18. Vandelli M, Fresta M, Puglisi G, Forni F (1994) J Microencapsul 11:531
19. Ming WH, Jones FN, Fu SK (1998) Polym Bull 40:749
20. Ming WH, Jones FN, Fu SK (1998) Macromol Chem Phys 199:1075
21. Winnik FM (1993) Chem Rev 93:587
22. Li M, Jiang M, Wu C (1997) J Polym Sci Pol Phys 35:1593
23. Wang YC, Winnik MA (1990) Langmuir 6:1437
24. Wilhelm M, Zhao CL, Wang YC, Xu RL, Winnik MA, Mura JL, Riess G, Croucher MD (1991) Macromolecules 24:1033
25. Okay O, Kay D, Pekcan O (1999) Polymer 40:6179
26. Hiemenz PC, Rajagopalan R (1997) Principles of colloid and surface chemistry, 3rd edn. Marcel Dekker, New York, pp 534–574
27. Sauzedde F, Ganachaud F, Elaissari A, Pichot C (1997) J Appl Polym Sci 65:2331
28. Charreyre MT, Revilla J, Elaissari A, Pichot C, Gallot B (1999) J Bioact Compat Polym 14:64
29. Wu Q, Xue Z, Qi Z, Wang F (2000) Synth Met 108:107